[From MEMOIRS of the School of Science & Engineering. No. 46 (1982) pp. 125~143]

On Stream Line Curved Beams

By

GENGO MATSUI

WASEDA UNIVERSITY

MEMOIRS OF THE SCHOOL OF
SCINCE & ENGINEERING
WASEDA UNIV. NO. 46, 1982

On Stream Line Curved Beams

GENGO MATSUI*

In orthogonal curved beam structures designed by Nervi and others, the beam arrangement always followed the direction of principal bending moments of an isotropic plate and beams of identical cross section were used uniformly, in the whole slab. However, for the main part of the plate the principal bending moments are not the same and consequently this concept does not result in an economical design.

In this paper, we propose a curved beam structure which comprises of main girders which carry the total roof load and sub-girders which prevent torsion of the main girders. Moreover, we seek to show the analogy which exists between the stream lines of a two dimensional fluid, the deflection contour lines of a stressed membrane, and the system of girders proposed hereafter.

A theoretical solution is arrived at for the stream lines by using complex functions, and the results of our experiments carried out on stressed membranes by using Moiré technics are also presented. A substantial part of this paper is devoted to reporting various examples of design in which this stream line beam structure is applied.

1. INTRODUCTION

There are two basically different types of rectangular cross beam systems consisting either of: (1) main and sub-girders, or (2) equivalent beams. In the first case, the total load is carried onto the supports by the main (or primary) girders, while the sub-girders only provide lateral support for the main girders, thus which are referred to as secondary beams. This may be likened to the orthotropic plate model. In the second case, an equal role is played by girders in both directions and this is more similar to an isotropic plate model. Usually, rectangular cross beam systems are built in the "main-sub-girder" form and it is only in cases where the depth of the slab is to be limited that type two will be used, as type one is more rational and economical. This main-sub-girder concept will be applied to curved beam systems, in the present paper.

Several orthogonal curved beam system designs are well known (*e.g.* the works of Nervi, S. Aoki, etc.). The beam arrangement in all of these cases conforms to the principal bending moment directions of the isotropic plate, and according to the isotropic plate hypothesis, every beam is built with the same concrete cross section throughout the slab. Figure 1 shows the Mohr's circle of bending moment, with M_1 and M_2 denoting the principal bending moments. In general, $M_1 > M_2$ and it is only in exceptional points that the Mohr's circle degenerates to one point. The design of uniform beams with the same concrete cross section

Received Sep. 24, 1982
* Department of Architecture.

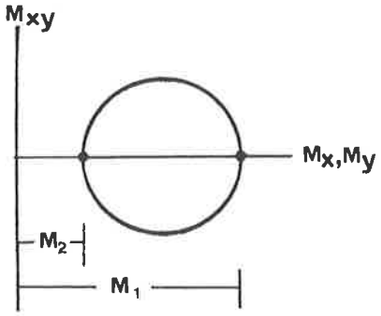

Fig. 1 Mohr's circle of bending moment for plate.

throughout the slab is consequently believed to be uneconomical.

In this paper, we consider a curved beam system which consists of main and sub-girders. Main girders function as primary beams carrying the total roof load onto the supports, and the sub-girders behave as secondary beams carrying the load between two primary beams, and additionally provide lateral support to them.

2. STREAM LINE CURVED BEAM[1)]

In the plane xy, a group of curves of direction α and an other one of direction $\beta = \alpha + 90$ represent respectively the primary and secondary beam directions. By denoting the shear resultant as Q_α and Q_β, then in accordance with the previous considerations, $Q_\beta \doteqdot 0$. That is to say, the whole load "goes" in the direction α of the primary beams.

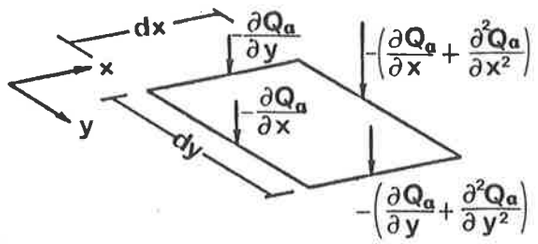

Fig. 2 Load in infinitesimal portion of beam.

In Fig. 2, a portion $dx\,dy$ of the field described above is depicted. Such a portion must necessarily be chosen as it is crossed by a primary beam. Since the negative differential of the shear force gives load, the values of load at the left and upper edges of the portion are $(-\partial Q_\alpha/\partial x)$, and $(-\partial Q_\alpha/\partial y)$ respectively, and the differential changes at the opposite edges are $(-\partial^2 Q_\alpha/\partial x^2)$, and $(-\partial^2 Q_\alpha/\partial y^2)$, respectively. Thus, the total differential of load on the element is: $-(\partial^2 Q_\alpha/\partial x^2 + \partial^2 Q_\alpha/\partial y^2)\,dx\,dy$. If the load is uniformly distributed, the above differential becomes zero, and we thus arrive at:

$$\frac{\partial^2 Q_\alpha}{\partial x^2} + \frac{\partial^2 Q_\alpha}{\partial y^2} = 0,$$

which is the second order Laplace's equation. Solving this equation, the curves $Q_\alpha = \text{const.}$ indicate the direction of the secondary beams, and the orthogonal direction is that of the primary beams.

In the two dimensional hydrodinamics, the velocity potential ϕ satisfies the same Laplace's equation:

$$\frac{\partial^2 \phi}{\partial x^2} + \frac{\partial^2 \phi}{\partial y^2} = 0,$$

and the stream lines are orthogonal to the solution $\phi = \text{const.}$ Consequently, the direction of the primary beams correspond to that of the streaming fluid.

Also, the deflection z of a stressed membrane satisfies the Laplace's equation:

$$\frac{\partial^2 z}{\partial x^2} + \frac{\partial^2 z}{\partial y^2} = 0$$

Thus the contour lines of its deflection give the direction of the secondary beams, while the orthogonal direction is that of the primary beams. In the present work, we have made use of this latter analogy, as the membrane experiment was easy to carry out. The membrane deflections were measured by the Moiré technics. In this method, the contour lines of deflection appear as strips (Moiré fringes), which are easy to observe.

3. STREAM LINE BEAM SYSTEMS WITH REGULAR POLYGONAL BOUNDARIES[2)]

In the case of a field with regular polygonal boundary, it is sufficient only to investigate one triangular portion which is formed by the borders of two neighbouring radii and one section of the boundary polygon (see Fig. 3).

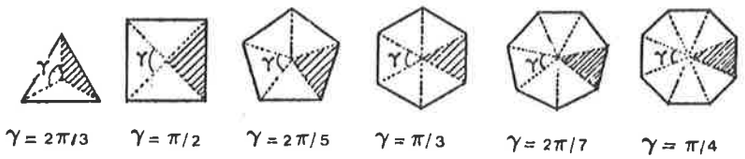

Fig. 3 Regular polygonal plates and radial lines (dashed lines) on which shear forces = 0.

3.1 Square boundary

In Fig. 4, the coordinate axes $x = 0$, and $y = 0$ are lines of primary beam; thus the maximum shear force at the mid-point of the boundary section is $w \cdot b$ (w: load/unit area). We assume that its value varies linearly, and is zero in the corners.

Investigating the triangular portion bordered by two dashed lines and one section of boundary, we find the solution for Q_α as the real part u of the complex function $f(z)$ which is defined as follows:

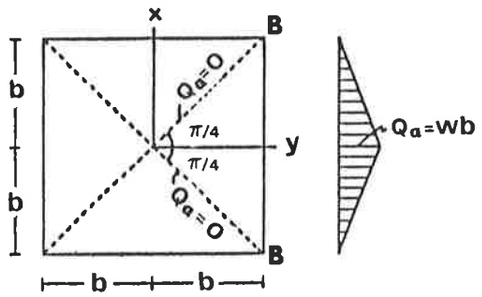

Fig. 4 Boundary condition of square plate.

$$f(z) = A_n \cdot z^{2n}, \quad n = 1, 3, 5, \cdots \quad (A_n \to \text{const})$$
$$f(z) = u + i \cdot v, \quad z = x + i \cdot y = r \cdot e^{i\theta},$$

In the curvilinear coordinates, u takes the form:

$$u = A_n \cdot r^{2n} \cdot \cos 2n\theta, \quad n = 1, 3, 5, \cdots$$

assuming zero values at $\theta = \pm\pi/4$. In the rectangular coordinate system xy, taking into account only two terms of the series:

$$u = A_1(x^2 - y^2) + A_3(x^6 - 15x^4y^2 + 15x^2y^4 - y^6)$$

For boundary conditions we can write:

$$\text{at } x = b,\ y = 0\text{: } u = Q_\alpha = wb$$
$$\text{at } x = b\text{: } \int_0^b u \cdot dy = wb^2/2$$

Hence

$$A_1 = (69/76)w/b, \quad A_3 = (7/76)w/b^5,$$

thus

$$Q_\alpha = \left(\frac{w}{76}\right) \cdot [69(x^2 - y^2)/b + 7(x^6 - 15x^4y^2 + 15x^2y^4 - y^6)/b^5]$$

and its value on the axis x is

$$Q_\alpha = \left(\frac{w}{76}\right) \cdot (69x^2/b + 7x^6/b^5)$$

This is plotted in Fig. 5. In the experiment, the frame of the membrane was formed from standing-triangular shaped edge members, while the height along its diagonals was zero, as it may be seen in Fig. 4. The values of height obtained from the Moiré fringes (see Fig. 6) are depicted by dot marks in Fig. 5 and, as can be seen, conform well to the present theory.

Since these Moiré fringes represent secondary beams the primary beams are obtained by drawing the orthogonal trajectories, as shown in Fig. 7. For comparison, we also give the direction of principal bending moments for an isotropic plate, in Fig. 8, which is quite similar to Fig. 7.

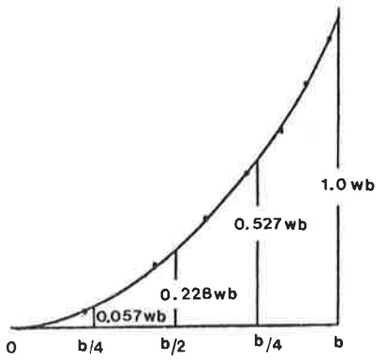

Fig. 5 Shear resultant on the x axis.

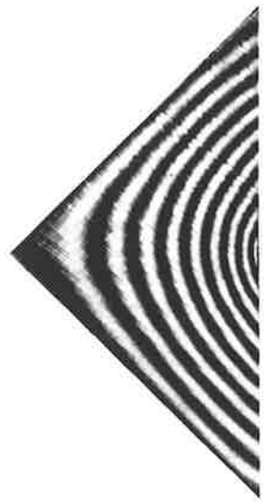

Fig. 6 Moiré fringes of square boundary.

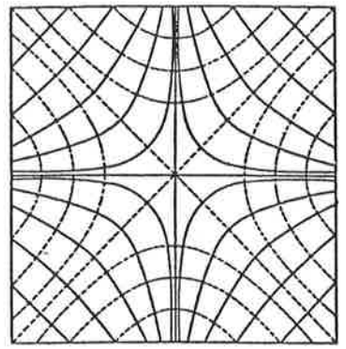

Fig. 7 Stream line beams for square plate.

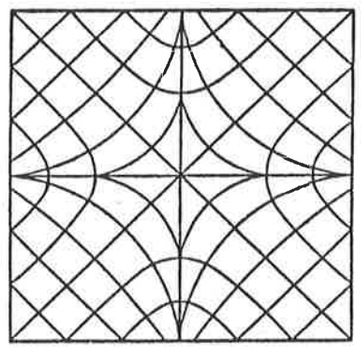

Fig. 8 Principal bending directions of square plate.

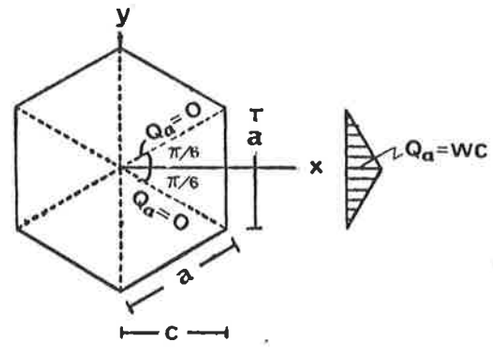

Fig. 9 Boundary condition of requlor hexagonal plate.

3.2 Hexagonal boundary

The coordinate system and one triangular portion of the hexagonal field bordered by two dashed lines and one section of boundary are shown, in Fig. 9. The solution for Q_α is obtained as the real part u of the complex function $f(z)$:

$$f(z) = A_n \cdot z^{3n}, \quad n = 1, 3, 5, \cdots$$
$$u = A_n \cdot r^{3n} \cdot \cos 3n\theta$$

The real function u assumes zero values at $\theta = \pm\pi/6$. In the coordinate system xy, considering only two terms of the series

$$u = A_1 x(x^2 - 3y^2) + A_3 x(x^8 - 36x^6y^2 + 126x^4y^4 - 84x^2y^6 + 9y^8)$$

The boundary conditions are:

$$\text{at } x = c,\ y = 0\text{: } u = \sqrt{3} \cdot aw/2$$
$$\text{at } x = c\text{: } \int_0^{a/2} u \cdot dy = \sqrt{3} \cdot aw/8$$

Hence,

$$A_1 = (917/789) \cdot w/a^2, \quad A_3 = (320/789) \cdot w/a^8$$

The shear resultant on the axis x assumes the form:

$$Q_\alpha = (w/789) \cdot [917x^3/a^2 + 320x^9/a^8]$$

This result is shown by the curve, and those derived from the Moiré experiment (see Fig. 10) are depicted by the dot marks, in Fig. 11. The stream line beams are seen in Fig. 12. For comparison, in Fig. 13, we also give the principal bending directions for an isotropic plate computed by the finite element method. This differs somewhat from Fig. 12.

3.3 Triangular boundary

The position of the triangle in the coordinate system is shown, in Fig. 14. The complex function $f(z)$ is defined as:

$$f(z) = A_n \cdot z^{(3/2)n}, \quad n = 1, 3, 5, \cdots$$

and its real part u is:

$$u = A_n \cdot r^{(3/2)n} \cdot \cos \frac{3}{2} n\theta,$$

assuming zero values at $\theta = \pm\pi/3$. The boundary conditions in the points A and B, respectively are: $u = w \cdot c$, and $u = 2w \cdot c/3$. Considering only two terms of the series:

$$A_1 = 1.685w/a^{1/2}, \quad A_3 = 7.327w/a^{7/2}$$

and the value of the shear resultant on the axis x:

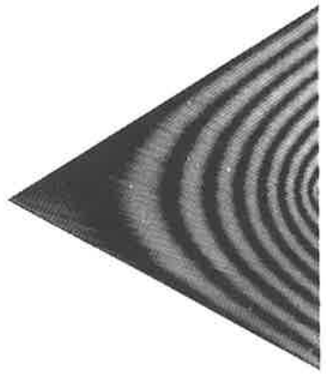

Fig. 10 Moiré fringes of regular hexagonal boundary.

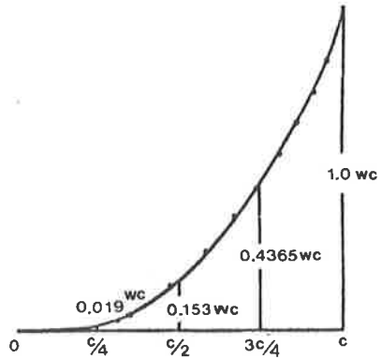

Fig. 11 Shear resultant on the x axis.

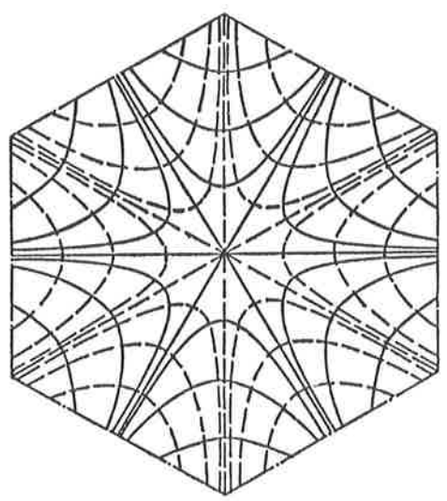

Fig. 12 Stream line beams for regular hexagonal plate.

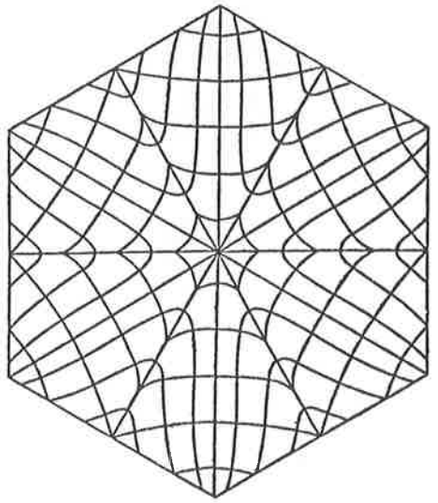

Fig. 13 Principal bending directions of isotropic regular hexagonal plate.

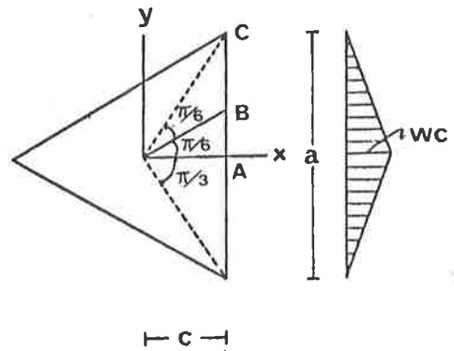

Fig. 14 Boundary condition of equilateral triangular plate.

$$Q_\alpha = (1.685w/a^{1/2})\cdot x^{3/2} + (7.327w/a^{7/2})x^{9/2}$$

In Fig. 16, this result is shown by the curve, and those obtained from the Moiré experiment (see Fig. 15) are depicted by the dot marks. Figures 17 and 18 show the stream line beams and the principal bending directions of an isotropic plate, respectively. The two figures are quite different, especially at the middle of the boundary section.

Fig. 15 Moiré fringes of equilateral triangular boundary.

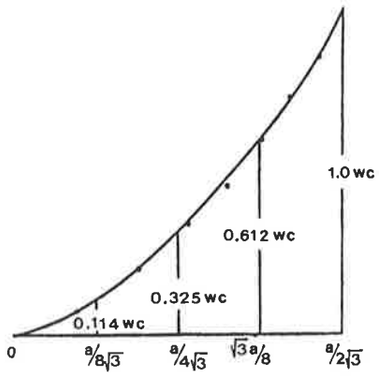

Fig. 16 Shear resultant on the axis x.

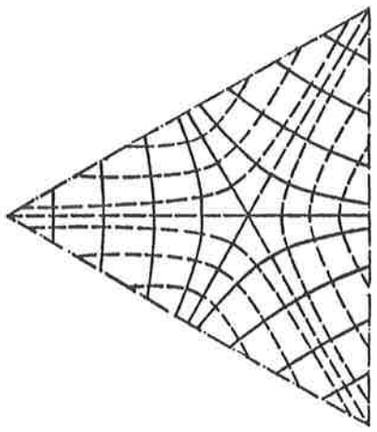

Fig. 17 Stream line beams for equilateral triangular plate.

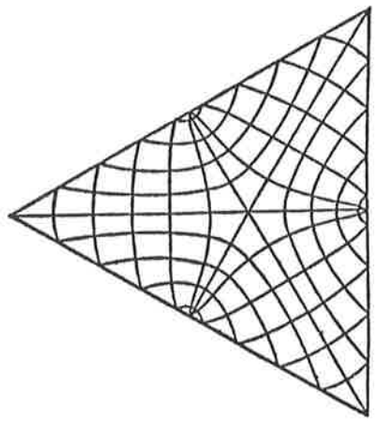

Fig. 18 Principal bending directions of isotropic equilateral triangular plate.

3.4 Pentagonal boundary

In this case, the complex function $f(z)$ is defined as:

$$f(z) = A_n\cdot z^{(5/2)n}, \quad n = 1, 3, 5, \cdots$$

The boundary conditions are given in Fig. 19. Finally, the shear resultant on the axis x assumes the function:

$$Q_\alpha = (1.513w/a^{3/2})x^{5/2} + (1.541w/a^{13/2})x^{15/2}$$

which is plotted, in Fig. 21. Also, the results obtained from the Moiré experiment (see Fig. 20) are shown by dot marks, in the same figure. The stream line beams are given in Fig. 22.

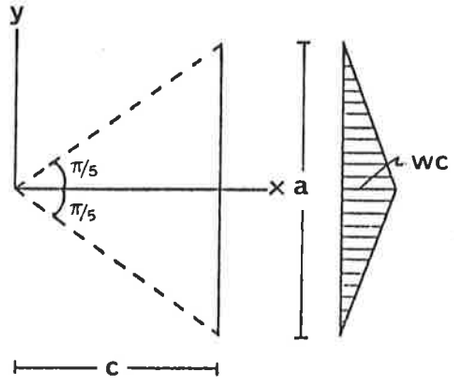

Fig. 19 Boundary condition of regular pentagonal plate.

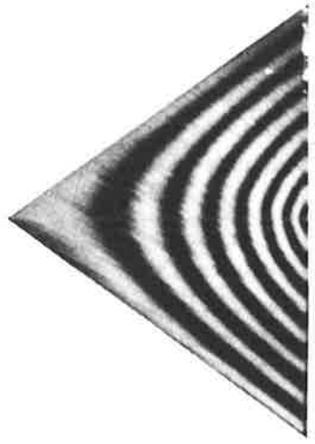

Fig. 20 Moiré fringes of regular pentagonal boundary.

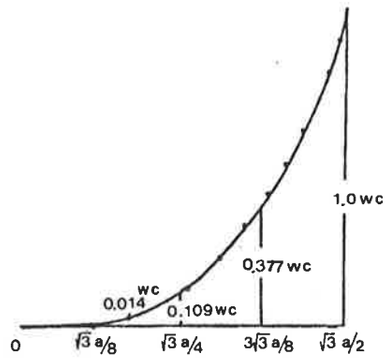

Fig. 21 Shear resultant on the x axis.

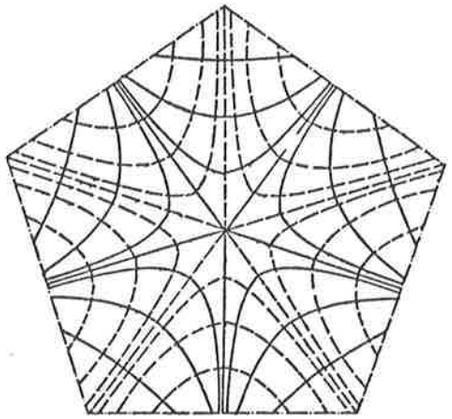

Fig. 22 Stream line beams for requlars pentagonal plate.

4. DESIGN EXAMPLES FOR POLYGONAL BOUNDARY

4.1 Hongkong Project, Indoor Stadium (Proposal)

Figure 23 shows the plan of this stadium: the steel structure of the roof being supported by reinforced concrete stands. The roof which measures 95 m × 95 m is formed out of steel beams which are arranged in conformity with the square stream line system discussed in section 2.1. The weight of the roofing is 300 kg/m^2. The weight of the steel structure, in this proposal, is 1700 t which may be contrasted to the value exceeding 2000 t, which is necessary in the case of the widely accepted, diagonally placed cross beams. This difference in steel quantity originates mainly from the fact that in our proposal lattice is unnecessary in the secondary beams. (Figure 24 shows a model of this roof structure.)

4.2 Gymnasium in Ueda City

This gymnasium also has a steel roof and reinforced concrete lower structures. The beam arrangement in the roof which is 50 m × 50 m conforms to the square stream line system (see Fig. 25). An interior view of the completed building may be seen, in Fig. 26.

4.3 Gakushuin High-School Gymnasium

This gymnasium is relatively small, and its roof which measures 31 m × 34 m is formed by polygonal steel beams following the stream line system (Fig. 27). Figures 28 and 29 show photos which were taken by using a fish-eye lens, during the construction and after the completition of the building.

4.4 Cultural Center in Shibata (Proposal)

The roof of the auditorium is a 27 m × 27 m steel structure of hexagonal shape, as seen

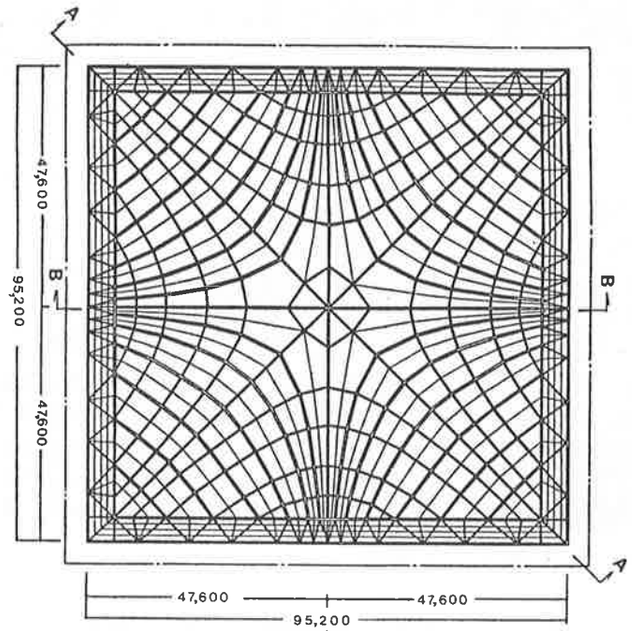

Fig. 23 Hongkong project, Indoor stadium.

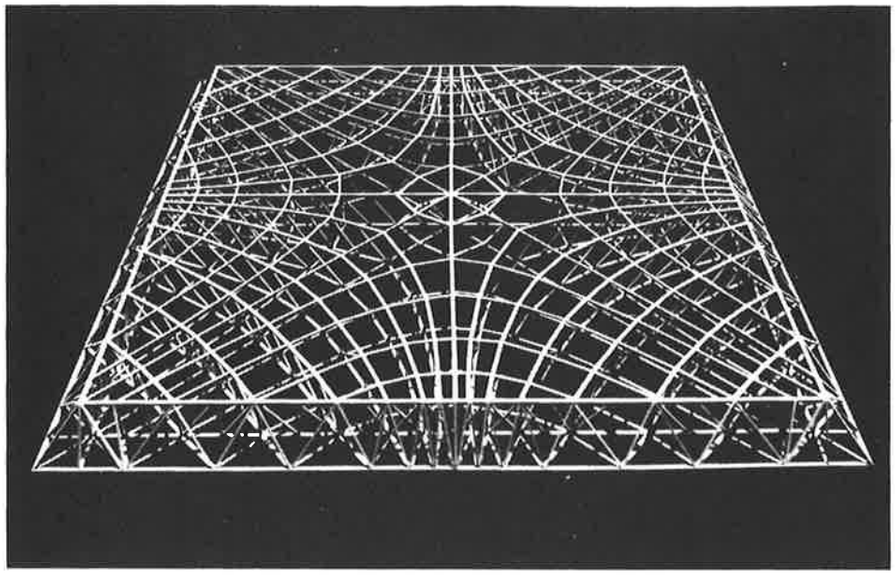

Fig. 24 Model of roof structure in Hong-Kong indoor stadium.

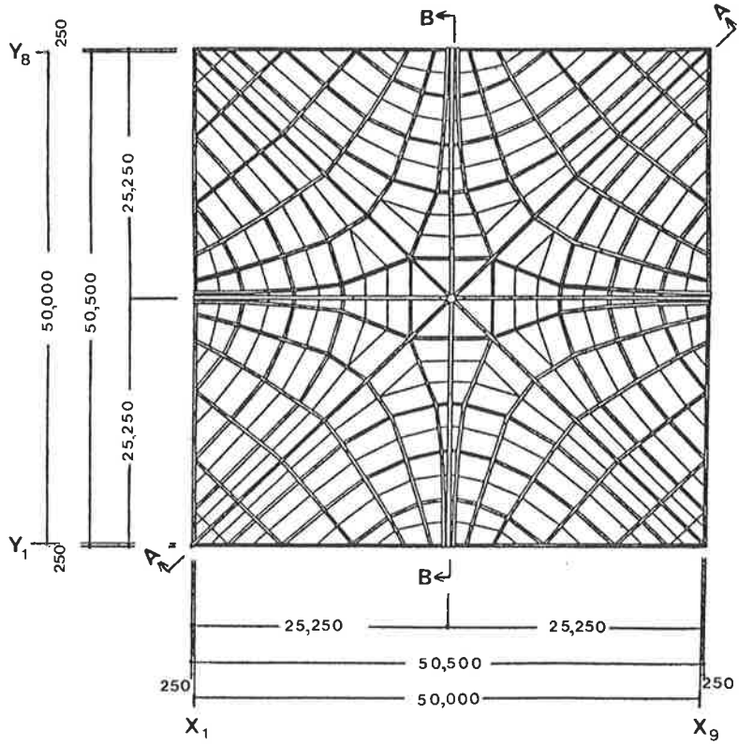

Fig. 25 Beam plan of gymnasium in Ueda City.

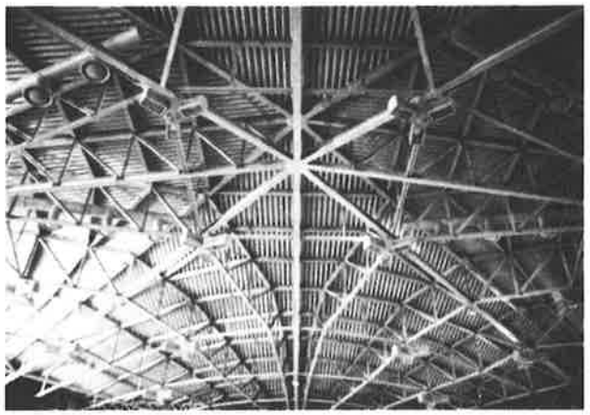

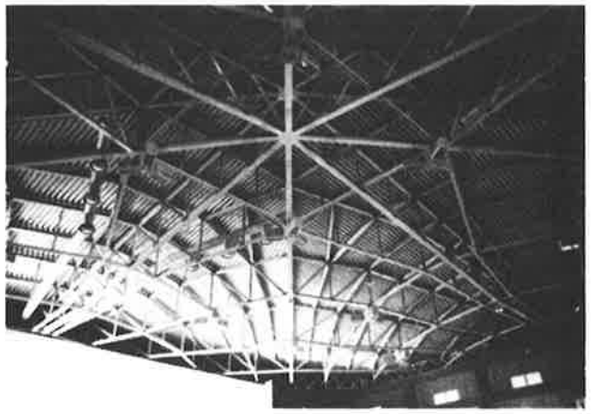

Fig. 26 Gymnasium in Ueda City.

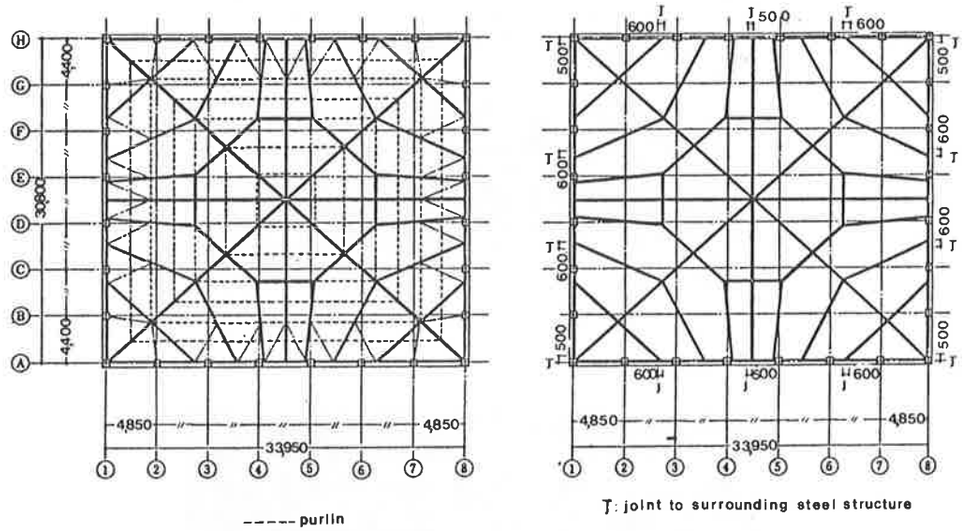

Fig. 27 Beam plan of Gakushuin High-school gymnasium.

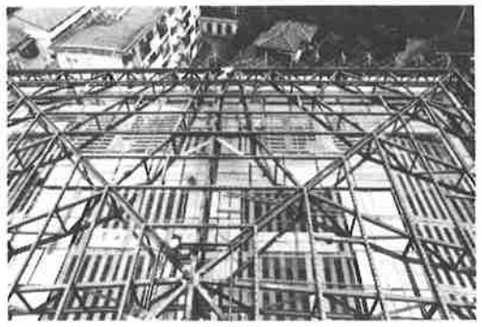

Fig. 28 Gakushuin High-School gymnasium roof structure under construction.

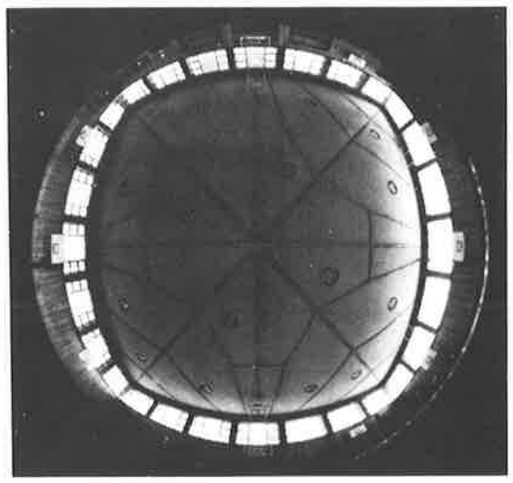

Fig. 29 Fish's-eye view of Gakushuin High-School gymnasium.

in Fig. 30. Figure 31 shows a picture of its model test. In Figs. 32 and 33, the stream line beam system, and simplified polygonal beams adopted in the design are shown, respectively.

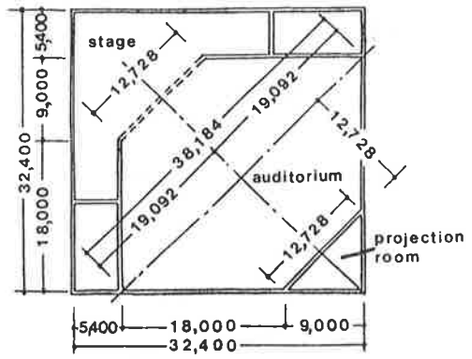

Fig. 30 Cultural center in Shibata City.

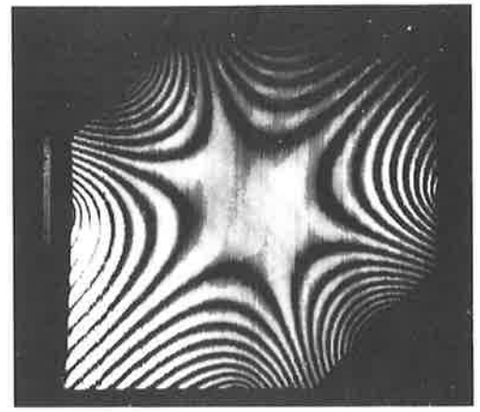

Fig. 31 Moiré fringes of roof model of Cultural Center in Shibata City.

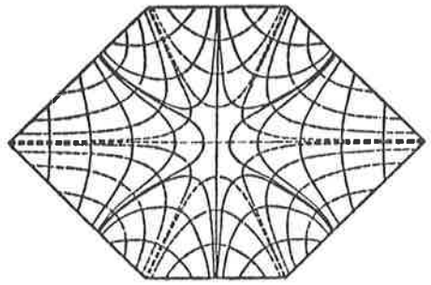

Fig. 32 Stream line beam system

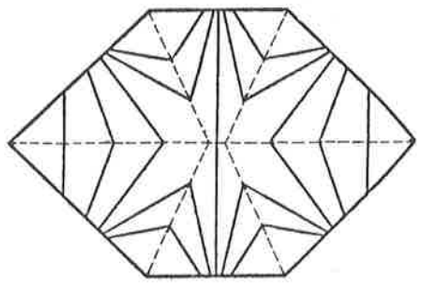

Fig. 33 Simplified polygonal beams of design.

5. HYPERBOLIC BEAM ARRANGEMENT

The plan of the dining hall of the Hotel New Akao in Atami is shown in Fig. 34. This semicircular-like building has one floor under and one floor above the ground. Due to environmental landscape requirements it was built with a flat roof which was covered by earth and planted with trees. Figure 35 shows the version of solution using cross beam roof structure, whereby the bending moments alter vaguely, and no clear distinction between main and sub-girders is apparent.

In Fig. 36, one can see the stream lines (full line), and the potential curves (dashed line) in the vicinity of an opening. The stream lines turn in-around, as the fluid passes through the opening. Figure 37 shows the beam plan of the roof that was set up in consideration of the above stream line system. That is to say, the primary and secondary beams follow the

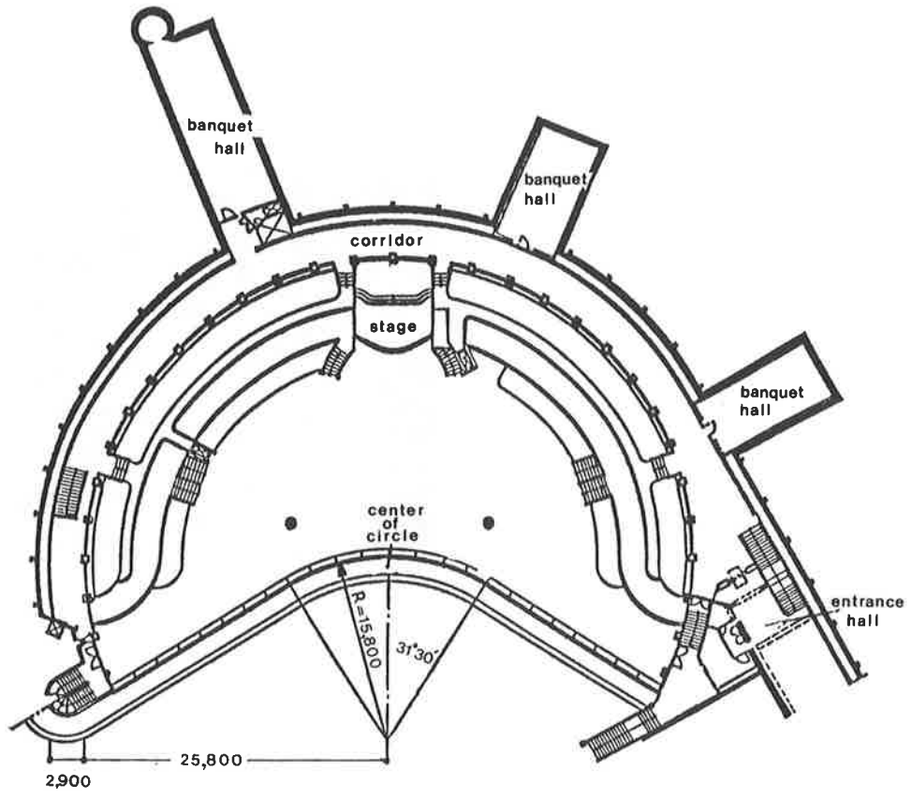

Fig. 34 Main dining hall of Hotel New Akao.

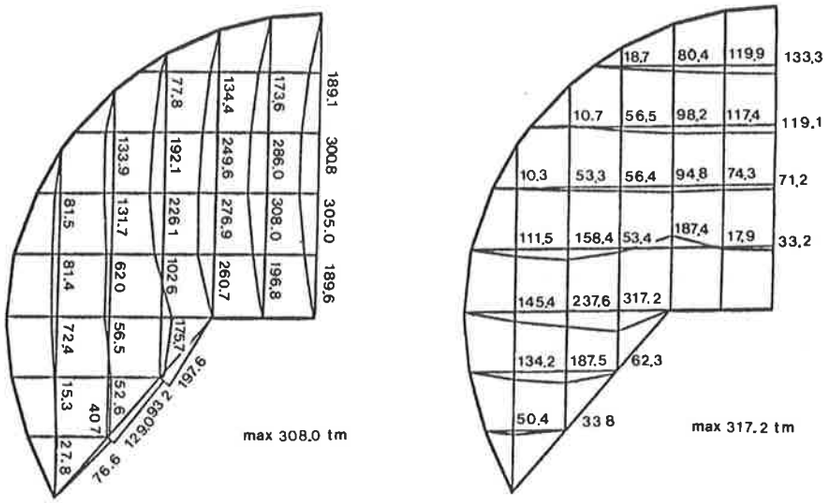

Fig. 35 Bending moments of cross beam roof structure.

stream lines and the potential curves, respectively. The bending moments of this curved beam system are given in Fig. 38. It is clear from this, that it is the primary beams which fulfill the role of carrying load onto the supports.

In construction, the main girders (primary beams) were made of a steel-reinforced concrete composite structure, and the sub-giders (secondary beams) were made of reinforced concrete. Figure 39 is a bird's-eye view of the roof under construction at the stage when the steel girders were set up in place. Figure 40 shows an inner view of the completed hall: the stream line beams having been left exposed in the interior.

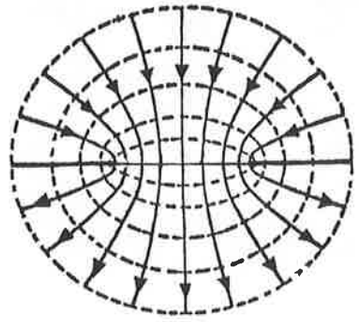

Fig. 36 Stream lines (full line) and potential curves (dashed line) in the vicinity of an opening.

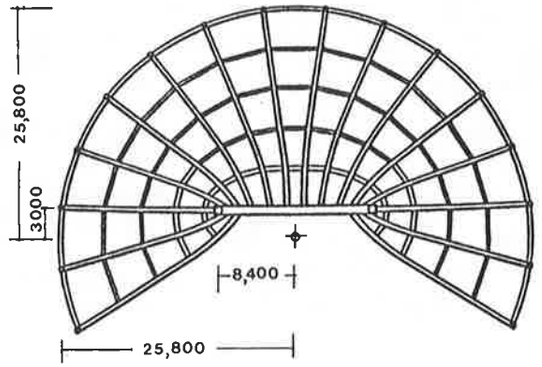

Fig. 37 Beam plan of the main dining hall.

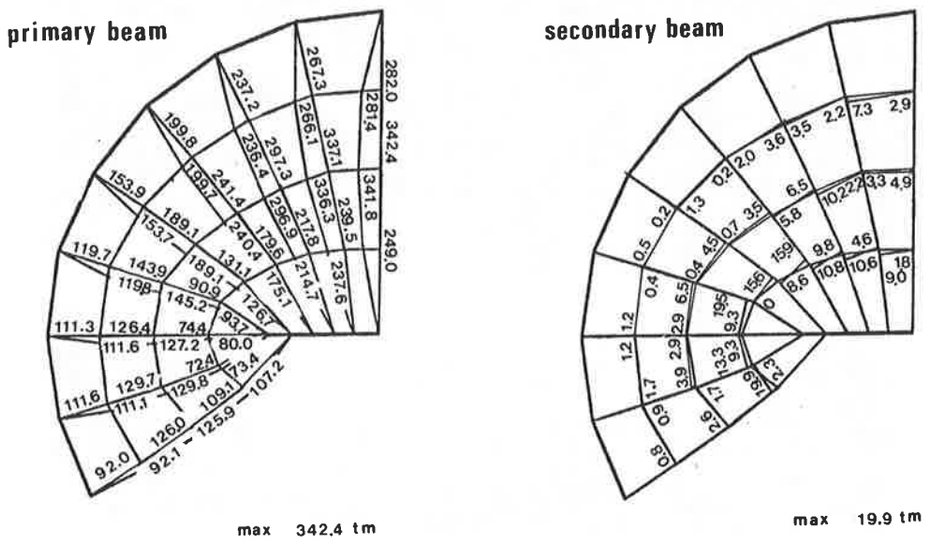

Fig. 38 Bending moments of the curved beam system.

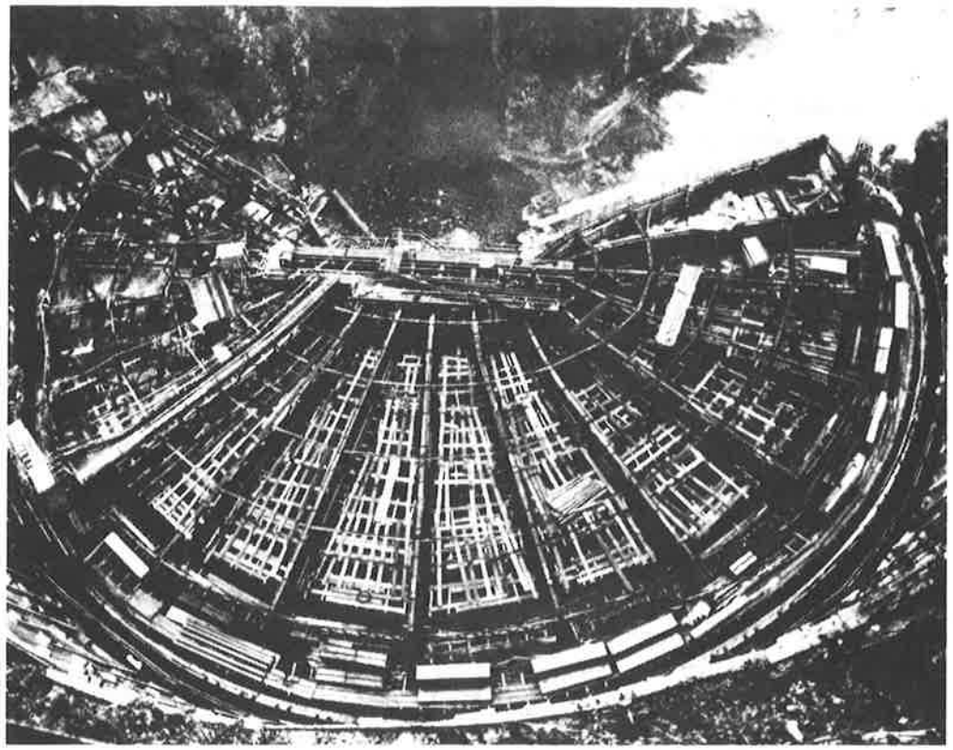

Fig. 39 Bird's-eye view of roof structure of main dining hall under construction.

Fig. 40 Inner view of main dining hall of Hotel New Akao.

References

1) Matsui: Pattern of One-Way Curved Beam System and Its Application. Transactions of the Architectural Institute of Japan, March, 1976.
2) Matsui: One-Way Curved Beam System with Regular Polygonal Boundary. Transactions of the Architectural Institute of Japan, January, 1977.
3) Salvadori, Heller: Structure in Architecture, pp. 241, Prentice-Hall, 1963.
4) Timoshenko, Woinowski-Krieger: Theory of Plates and Shells, pp. 313, McGraw-Hill, 1959.